



# Synthesis, X-Ray Crystallography, Theoretical Investigation and Optical Properties of 2-Chloro-*N*-(2,4-dinitrophenyl) Acetamide

Piangkwan Jansukra<sup>1</sup> · Worawat Wattanathana<sup>2</sup> · Tanwawan Duangthongyou<sup>1</sup> · Suttipong Wannapaiboon<sup>3</sup> · Apisit Songsasean<sup>1</sup> · Songwut Suramitr<sup>4,5</sup> · Thawatchai Tuntulani<sup>6</sup> · C. Scott Browning<sup>7</sup> · Boontana Wannalarse<sup>1</sup>

Received: 4 July 2020 / Accepted: 11 December 2020

© The Author(s), under exclusive licence to Springer Science+Business Media, LLC part of Springer Nature 2021

## Abstract

2-Chloro-*N*-(2,4-dinitrophenyl) acetamide, **1**, was synthesized and characterized by <sup>1</sup>H and <sup>13</sup>C NMR spectroscopy, ESI-MS, X-ray crystallography, and elemental analysis. This compound crystallizes in the monoclinic space group P2<sub>1</sub>/n. The crystal structure of compound **1** revealed the intramolecular H-bonding with the *S*(6) motif between H atom of the amide group and the nitro group at the *ortho* position. Several intermolecular C–H···O interactions hold different molecules of the compound **1** together resulting in the crystal packing. Red faint spots observed in the Hirshfeld surface of the compound **1** confirm the presence of N–H···O hydrogen bond as well as C–H···O interactions. According to the Hirshfeld surface, C–H···Cl interaction is also found, of which distance is relatively longer than the C–H···O distance. Moreover, the analysis of the corresponding fingerprint plots indicates the significant interactions within the crystal namely H···O/O···H (39.0%), C···O/O···C (10.6%), H···Cl/Cl···H (8.5%), H···H (7.3%), and H···C/C···H (5.9%) contacts. The optical properties of compound **1** in various solvents were investigated using UV–vis spectrophotometry. Compound **1** showed solvatochromic effects upon the varying polarity of the solvent. Time-dependent DFT calculations (TD-DFT) of compound **1** suggest that the deprotonation process occurs in polar solvents such as DMF.

✉ Boontana Wannalarse  
fscibnw@ku.ac.th

<sup>1</sup> Department of Chemistry and Center of Excellence for Innovation in Chemistry, Faculty of Science, Kasetsart University, Chatuchak, Bangkok 10900, Thailand

<sup>2</sup> Department of Materials Engineering, Faculty of Engineering, Kasetsart University, Chatuchak, Bangkok 10900, Thailand

<sup>3</sup> Synchrotron Light Research Institute (Public Organization), 111 University Avenue, Suranaree Sub-district, Muang, Nakhon Ratchasima 30000, Thailand

<sup>4</sup> Department of Chemistry, Faculty of Science, Kasetsart University, Chatuchak, Bangkok 10900, Thailand

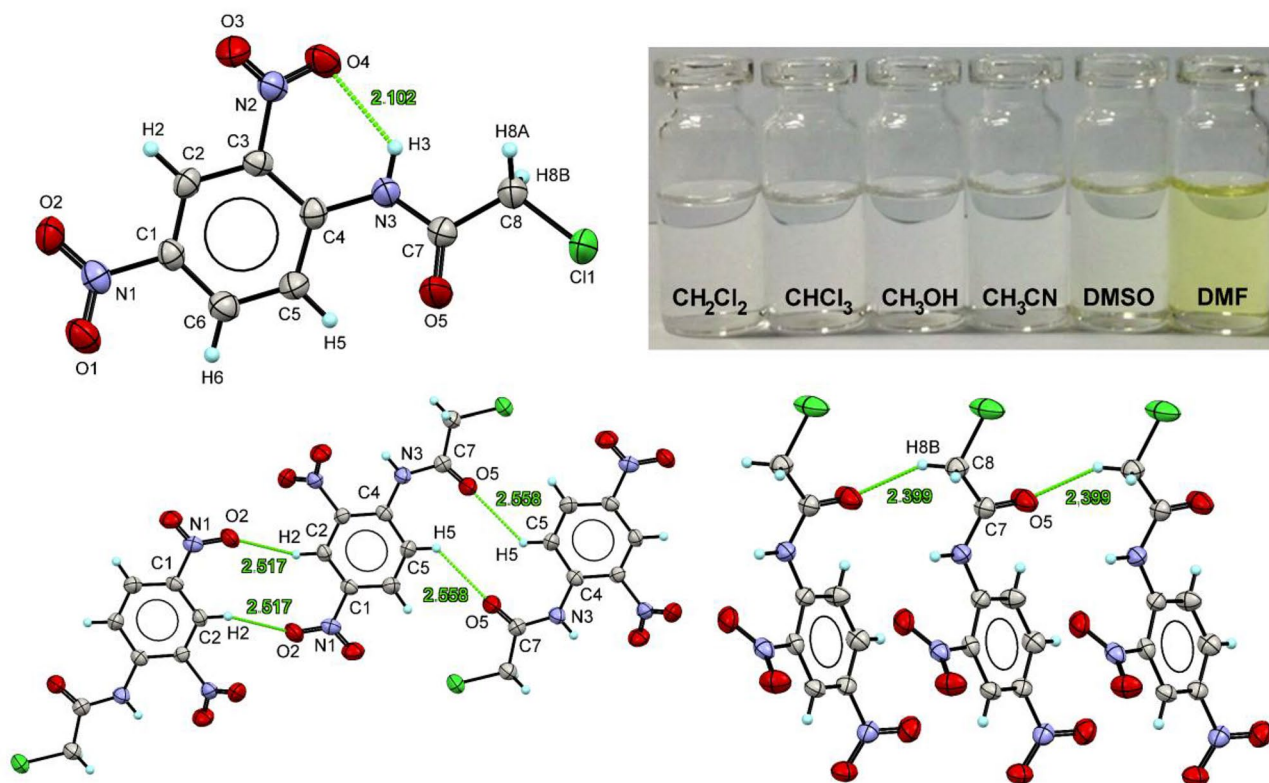
<sup>5</sup> Center for Advanced Studies in Nanotechnology for Chemical, Food and Agricultural Industries, KU Institute for Advanced Studies, Kasetsart University, Bangkok 10900, Thailand

<sup>6</sup> Supramolecular Chemistry Research Unit, Department of Chemistry, Faculty of Science, Chulalongkorn University, Bangkok 10330, Thailand

<sup>7</sup> Davenport Chemical Research Building, Department of Chemistry, University of Toronto, 80 St. George St., Toronto M5S 3H6, Canada

## Graphic Abstract

Crystal structure of 2-Chloro-*N*-(2,4-dinitrophenyl) acetamide (**1**) revealed the intramolecular N–H···O hydrogen bonding with the S(6) motif within the molecule as well as several intermolecular C–H···O interactions between molecules. Moreover, the compound **1** exhibited solvatochromic effects upon the varying polarity of the solvents.



**Keywords** Crystal structure · 2,4-Dinitroaniline derivative · Hydrogen bonding interactions

## Introduction

Dinitroaniline and its derivatives, which consist of both electron-donating and electron-withdrawing groups connected by a  $\pi$ -conjugated system, have received a great deal of attention in the field of optoelectronic devices. There are many types of dinitroaniline species having either a linear or non-linear arrangement of the electron-donating and withdrawing groups. They are employed to produce aggregated molecular structures in one (1-D), two (2-D), and three dimensional (3-D) networks via the intermolecular forces such as hydrogen bonding,  $\pi$ - $\pi$  stacking, CH- $\pi$  interactions, and van der Waal forces [1–6]. Furthermore, dinitroaniline derivatives are known as solvatochromic chromophores [7], possessing the color alteration by means of a variation of solvent polarities. Dinitroaniline and its derivatives may undergo several photophysical processes, including electron transfer (ET), internal charge transfer (ICT), and proton transfer (PT). The keto-enol isomerization is an example

of rapid photo-induced proton transfer in dinitroanilines, that varies in its extent with solvent polarity [8–14]. Many techniques, for example, IR,  $^1\text{H-NMR}$ , and UV-vis spectroscopies have been used to examine such proton transfer processes through the study of metastable intermediates forming during the process. However, it is quite difficult to investigate these molecules since it is difficult to terminate the reaction process at the formation of metastable intermediates and separates them for further spectroscopic characterizations. A TD-DFT calculation is a quick and facile method that can predict and optimize the energy level of these compounds [7, 15, 16]. Singh et al. synthesized isomeric hydrazone derivatives containing 2,4-dinitrophenyl hydrazone group, and studied the various electronic transition within a molecule in two different solvents (ethanol and dichloromethane) by UV-vis spectroscopy, DFT and AIM approach. The result indicates that these derivatives in two different solvents displayed the significant redshift in the spectrum stemming from characteristic

hydrogen bonding interaction between the derivatives and solvents. Moreover, their structures were stabilized by both the hyper-conjugation and the electron delocalization via the  $\pi$ -conjugated bridge, which consequently lead to the internal charge transfer (ICT) process [17].

This recent work describes the synthesis, characterization, and investigation of the optical properties of 2-chloro-*N*-(2,4-dinitrophenyl) acetamide (**1**) in various solvents using UV–vis spectrophotometry. The crystal structure of this compound is examined. TD-DFT calculations are used to support the study of the intramolecular proton transfer process of this compound in solution.

## Experimental

### General Information

$^1\text{H-NMR}$  spectrum was collected using a 400 MHz NMR spectrometer. UV–vis spectra were recorded on a Shimadzu spectrophotometer. Mass spectroscopy (MS) was carried out on an Agilent 1100 Series LC/MSD Trap mass spectrometer. Infrared spectra ( $4000\text{--}400\text{ cm}^{-1}$ ) were obtained from a Perkin Elmer system 2000 Fourier transform infrared spectrometer. A Buchi melting point B-540 analyzer determined the melting point of the sample. All solvents and reagents were purchased from Sigma Aldrich and used without further purification.

### Synthesis and Characterization

The synthesis route to prepare 2-chloro-*N*-(2,4-dinitrophenyl)acetamide is summarized in Scheme 1. Firstly, 2,4-dinitroaniline (2.0 g, 14.48 mmol) and triethylamine (4 mL, 28.96 mmol) in dichloromethane (3 mL) were stirred under  $\text{N}_2$  for 30 min. Then, solution of 2-chloroacetyl chloride (2.3 mL, 28.96 mmol) in dichloromethane (3 mL) was added dropwise to the mixture. The reaction mixture was continuously stirred for 24 h. The reaction mixture was poured into water and extracted with dichloromethane (3 times). The organic layer was dried with anhydrous  $\text{Na}_2\text{SO}_4$ . 2-Chloro-*N*-(2,4-dinitrophenyl)acetamide, **1**, was purified by column chromatography using dichloromethane as an eluent to give a yellow solid (0.56 g, 19.6%). The yellow crystals were obtained by

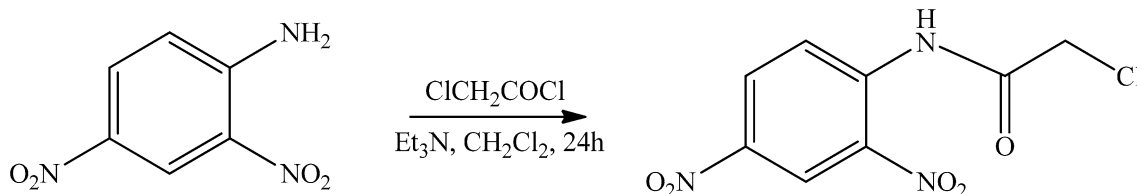
recrystallization in a mixture of dichloromethane/hexane (1:1 v/v). m.p. 116.5 °C. IR (KBr,  $\text{cm}^{-1}$ ): 3328, 1686, 1604, 1511, 1343, 1227, 593  $^1\text{H NMR}$  (400 MHz,  $\text{CDCl}_3$ ):  $\delta$  11.77 (s, 1H, -NH), 9.18 (d,  $J=6.9$  Hz, 1H, -ArH), 9.11 (d,  $J=8.4$  Hz 1H, -ArH), 8.59 (d,  $J=7.1$  Hz, 1H, -ArH), 4.45 (s, 2H,  $-\text{CH}_2$ ).  $^{13}\text{C NMR}$  (100 MHz,  $\text{CDCl}_3$ ): 165.7, 142.6, 140.1, 136.4, 128.9, 124.9, 121.3, 43.1 ESI-MS:  $m/z$  260.0  $[\text{M} + \text{H}^+]$  Elemental Anal: Calcd for  $\text{C}_8\text{H}_6\text{N}_3\text{O}_5\text{Cl}$ : C, 37.01; H, 2.33; N, 16.19 Found: C, 37.03; H, 2.28; N, 16.09.

### Crystallography

Single crystal data of compound **1** were collected at 276 K on a Bruker APEXII CCD camera by  $\Psi$  and  $\omega$  scans using graphite-monochromated radiation ( $\text{MoK}\alpha$ ,  $\lambda=0.71073\text{ \AA}$ ). Reflections of the single crystal were measured in a  $2\theta$  range of  $2.0^\circ\text{--}25.1^\circ$ , and 1740 independent reflections were measured for compound **1**. The structure solution and refinement were performed using Olex2 software [18]. The structure was solved by the intrinsic phasing method using the SHELXT program [19] and was then refined by full-matrix least-squares using SHELXL package [20]. Non-hydrogen atoms were isotropically refined at first and refined anisotropically to obtain their thermal parameters. All hydrogen atoms of compound **1** apart from H3 were treated anisotropically while the H atoms were refined by a riding model with  $d(\text{C-H})=0.95\text{ \AA}$  and  $U_{\text{iso}}(\text{H})=1.2U_{\text{eq}}(\text{C})$  for aromatic hydrogen atoms, with  $d(\text{C-H})=0.99\text{ \AA}$  and  $U_{\text{iso}}(\text{H})=1.2U_{\text{eq}}(\text{C})$  for  $-\text{CH}_2-$  hydrogen atoms and  $d(\text{C-H})=0.98\text{ \AA}$ ,  $U_{\text{iso}}(\text{H})=1.5U_{\text{eq}}(\text{C})$  for the terminal methyl hydrogen atoms. located from a different Fourier map and refined. The final least-square cycle of refinement gave out  $R_1=0.0391$  and  $wR_2=0.0956$ . The crystal data and refinement details of compound **1** are listed in Table 1. Mercury software is used to acquire molecular graphics for this manuscript [21].

### Computational Details

The optimized structure of compound **1** obtained from X-ray diffraction data was calculated using the density functional theory (DFT) level of CAM-B3LYP [22] with a 6-311G(d,p) basis set using Gaussian 09 program [23]. A polarizable-continuum model (PCM) [24] was employed for



**Scheme 1** The synthesis pathway of 2-chloro-*N*-(2,4-dinitrophenyl)acetamide, **1**

**Table 1** Crystallographic data and structure refinement for compound **1**

CCDC number	1419554
Empirical formula	C <sub>8</sub> H <sub>6</sub> N <sub>3</sub> O <sub>5</sub> Cl
Formula weight	259.61
Temperature/K	296.15
Crystal system	Monoclinic
Space group	P2 <sub>1</sub> /n
a/Å	13.486 (2)
b/Å	4.6294 (7)
c/Å	16.081 (3)
α/°	90
β/°	92.245 (9)
γ/°	90
Volume/Å <sup>3</sup>	1003.2 (3)
Z	4
ρ <sub>calc</sub> /cm <sup>3</sup>	1.719
μ/mm <sup>-1</sup>	0.397
F(000)	528.0
Crystal size/mm <sup>3</sup>	0.48 × 0.08 × 0.05
Radiation	MoKα (λ = 0.71073)
2θ range for data collection/°	6.046–50.12
Index ranges	– 13 ≤ h ≤ 16, – 5 ≤ k ≤ 5, – 19 ≤ l ≤ 17
Reflections collected	5142
Independent reflections	1740 [R <sub>int</sub> = 0.0243, R <sub>sigma</sub> = 0.0300]
Data/restraints/parameters	1740/0/158
Goodness-of-fit on F <sup>2</sup>	1.049
Final R indexes [I ≥ 2σ (I)]	R <sub>1</sub> = 0.0391, wR <sub>2</sub> = 0.0956

the investigation of solute–solvent interactions in dimethylformamide (DMF). All tautomers were fully optimized in solution. Frequency calculations were performed on the optimized structures to confirm that these structures correspond to energy minima. To simulate the absorption spectra, the vertical excitation energies were calculated at the optimized tautomers obtained with a restricted planar structure for the ground state using the time-dependent DFT (TD-DFT) method [25, 26] with the CAM-B3LYP/6-311G(d,p) basis set.

## Results and Discussion

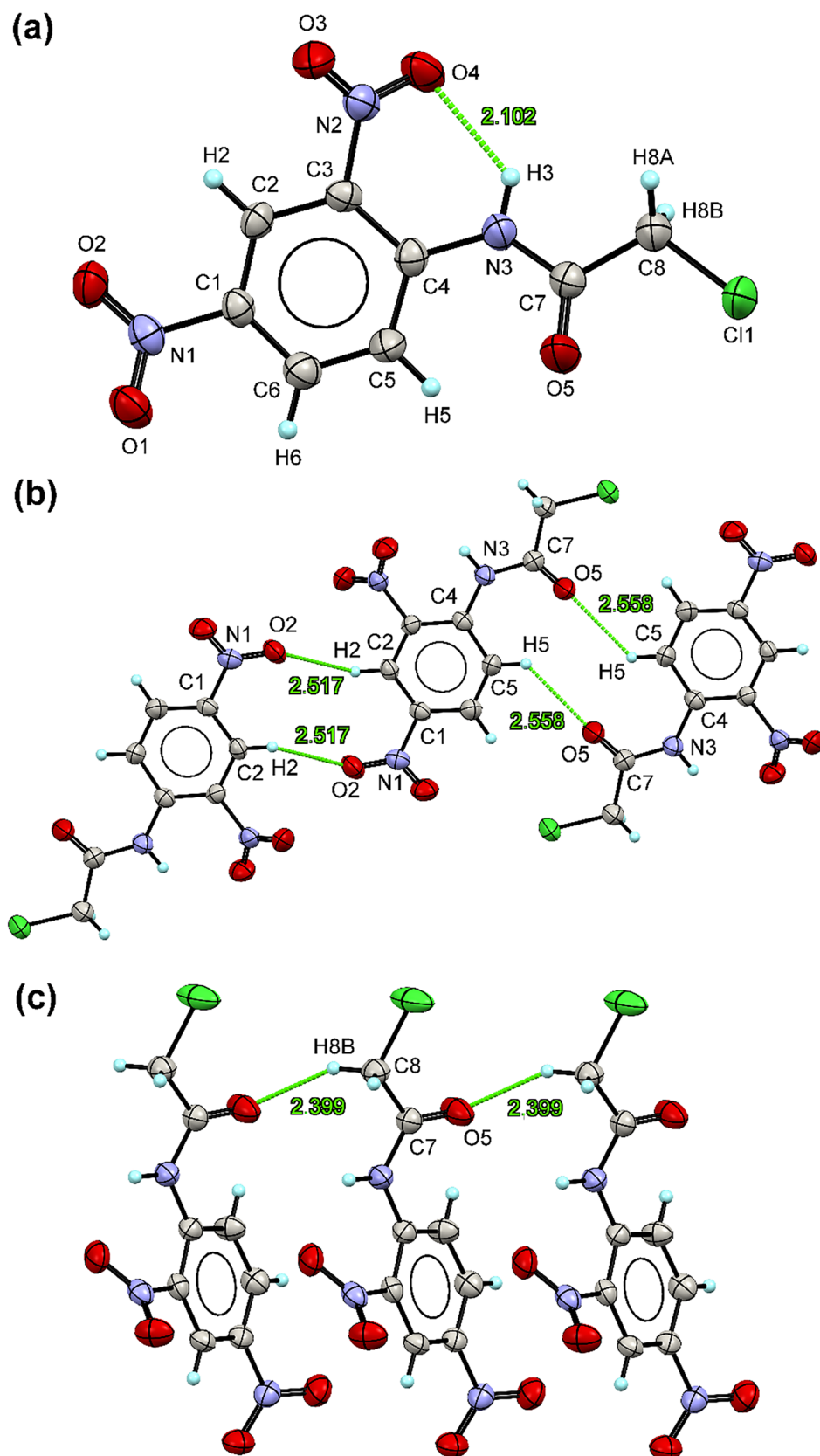
### Crystal Structure and Hirshfeld Surface Analysis

The ORTEP plot showing the molecular structure of compound **1** is displayed in Fig. 1a. Inspection of torsion angles of the peripheral groups attached to the benzene ring (Table 2) shows that neither two nitro groups nor the amide group is oriented coplanar with the benzene ring. Table 3 shows the selected bond lengths, bond angles and

torsion angles of compound **1** together with the structural parameters from the other 2-chlorophenylacetamide derivatives reported in the CSD database [27–29]. It was found that the significant bond lengths and bond angles regarding the nitro and 2-chloroacetamide groups in all the compounds are quite similar, but the torsion angles are different, depending on the substituent groups. Within the molecule of compound **1**, one of the oxygen atoms in the nitro group at the *ortho* position with respect to the amide group (O4) is twisted to locate near the H2 atom leading to the formation of an intramolecular hydrogen bond with *S*(6) motif from an O4–N2–C3–C4–N3–H3 synthon. The H atom (H3) regarding the *S*(6) graph set, which was refined freely, was found to locate at distances of 0.88 (3) Å and 2.10 (3) Å from N3 atom and O4 atom, respectively. The amide functional group adopts a *trans* conformation with the four atoms nearly coplanar, as shown by the O5–C7–N3–H3 torsion angle of 172 (2)°. From the literature survey of the related crystal structure, a number of 2-chloro-*N*-phenylacetamide derivatives can form a hydrogen bonding chain with the C(4) graph set via a secondary amide group (–NHC(=O)–) [28–34]. However, in our work, the compound **1** cannot create the C(4) intermolecular hydrogen-bonding chains to stabilize the crystal packing as the amide H is already used to form the intramolecular H-bond with an adjacent nitro substituent. Instead, several intermolecular C–H⋯O interactions with the H-acceptor distances < 2.6 Å are major contributors in crystal packing. Figure 1b illustrates two C–H⋯O interactions, C2–H2⋯O2, and C5–H5⋯O5, constructed from two inversion-related molecules of the compound **1**. The C2–H2⋯O2 and C5–H5⋯O5 interactions establish *R*<sub>2</sub><sup>2</sup>(8)- and *R*<sub>2</sub><sup>2</sup>(10)-like motifs. For the molecules related by mirror planes, the C–H⋯O interaction (C8–H8B⋯O) can also be found. The C8–H8B⋯O linkage joins the molecules of the compound **1**, giving rise to the infinite C(4)-like molecular chain. The full geometric parameters of the H-bond and C–H⋯O interactions are tabulated in Table 4.

The intermolecular interactions in the crystal of the compound **1** were investigated by performing a Hirshfeld surface (HS) analysis [35, 36] using *Crystal Explorer 17.5* [37]. The HS is plotted over the *d*<sub>norm</sub> range –0.2293 to 0.9126 a.u. (Fig. 2). Red faint spots confirm the presence of both the hydrogen bonding and C–H⋯O interactions mentioned earlier. Moreover, there are some more spots locate on H6 and C11 atoms. It might be due to the interactions with the H-acceptor distances more than 2.6 Å, such as C6–H6⋯C11 interaction. The study on the full two-dimensional fingerprint plot regarding the HS surface allows us to get a piece of insight information about the contribution of each contact to the crystal packing. The fingerprint plot can be delineated into the individual fingerprint plots for individual interactions [38]. Herein, the significant contacts within the crystal of the compound **1** are H⋯O/O⋯H (39.0%), C⋯O/O⋯C

**Fig. 1** **a** The molecular structure of the compound **1**, showing the atom-labelling scheme. Displacement ellipsoids are drawn at the 50% probability level. The non-IUPAC atom labelling is for the convenience of discussion. Crystal packing of the compound **1** showing C–H···O interactions formed from the molecules related by **b** inversion centers and **c** mirror planes



(10.6%), H $\cdots$ Cl/Cl $\cdots$ H (8.5%), H $\cdots$ H (7.3%), and H $\cdots$ C/C $\cdots$ H (5.9%) contacts (Fig. 3). The contributions of the other contacts are Cl $\cdots$ Cl (3.5%), O $\cdots$ Cl/Cl $\cdots$ O (5.3%), N $\cdots$ Cl/Cl $\cdots$ N (1.4%), C $\cdots$ Cl/Cl $\cdots$ C (1.2%), O $\cdots$ O (7.5%), N $\cdots$ O/O $\cdots$ N (5.0%), H $\cdots$ N/N $\cdots$ H (1.8%), C $\cdots$ N/N $\cdots$ C (0.7%), C $\cdots$ C (2.5%).

### The Study of the Solvatochromic Effect on 2-chloro-*N*-(2,4-dinitrophenyl)acetamide

2-Chloro-*N*-(2,4-dinitrophenyl)acetamide, **1**, consists of an amide group and two nitro groups on the aromatic ring. Compound **1** dissolves in several organic solvents (i.e., CH<sub>2</sub>Cl<sub>2</sub>, CHCl<sub>3</sub>, CH<sub>3</sub>CN, CH<sub>3</sub>OH, DMF, and DMSO). Solutions of **1** in different solvents showed a color variation ranging from

pale yellow to yellow with respect to an increase of solvent polarity, as shown in Fig. 4. The absorption spectra of **1** in various solvents are shown in Fig. 5. An absorption maximum is observed at 296–298 nm in solvents of low polarity (296 nm in CHCl<sub>3</sub>, 297 nm in CH<sub>2</sub>Cl<sub>2</sub>, 298 nm in CH<sub>3</sub>CN). In addition, the molar absorptions of compound **1** in different solvents can be calculated and listed in Table 5. As a highlight, the appearance of new absorption band at 425 nm suggests that the solvents of higher polarity induce a greater stabilization of the excited state than of the ground state, leading to the structural alteration of compound **1** [39]. This phenomenon is under the solvatochromism process [40, 41]. Using DMF and DMSO as solvent [42–46], there are two possible conformations of **1** in

**Table 2** Selected torsion angles

Torsion angle	Angle/°
O1–N1–C1–C2	– 151.3 (2)
O1–N1–C1–C6	28.9 (3)
O2–N1–C1–C2	28.3 (3)
O2–N1–C1–C6	– 151.5 (2)
O3–N2–C3–C2	33.3 (3)
O3–N2–C3–C4	– 144.7 (2)
O4–N2–C3–C2	– 146.9 (2)
O4–N2–C3–C4	35.1 (3)
C7–N3–C4–C3	147.5 (2)
C7–N3–C4–C5	– 30.2 (4)

**Table 4** Geometries of hydrogen bonds and C–H $\cdots$ O interactions in the crystal structure of the compound **1**

D–H $\cdots$ A	d(D–H)/Å	d(H–A)/Å	d(D–A)/Å	D–H–A/°
Hydrogen bond				
N3–H3 $\cdots$ O4	0.88 (3)	2.10 (3)	2.732 (3)	129 (3)
C–H $\cdots$ O interactions				
C2–H2 $\cdots$ O2 <sup>i</sup>	0.93	2.52	3.246 (3)	135
C5–H5 $\cdots$ O5 <sup>ii</sup>	0.93	2.56	3.227 (3)	129
C8–H8B $\cdots$ O5 <sup>iii</sup>	0.97	2.40	3.291 (3)	153

Symmetry codes: (i)  $-x, 1-y, 1-z$ ; (ii)  $1-x, 2-y, 1-z$ ; (iii)  $x, -1+y, z$

**Table 3** Comparison of bond lengths, bond angles and torsion angles of compound **1** and other 2-chlorophenylacetamide derivatives reported in the CSD database

Crystal data	This work	Ref. [27]	Ref. [27]	Ref. [28]	Ref. [29]
Ref. code	–	CAKVAO	CAKVES	REZPES	WEPKOS
CCDC no.	1419554	723202	723202	613384	624978
Bond length (Å)					
N2–C3	1.456 (3)	1.4709 (16)	1.4679 (13)	1.452 (6)	1.467 (3)
N2–O3	1.225 (3)	1.2343 (14)	1.2286 (12)	1.203 (5)	1.214 (2)
N2–O4	1.225 (3)	1.2215 (15)	1.2232 (13)	1.233 (5)	1.229 (2)
N3–C4	1.399 (3)	1.4178 (15)	1.4124 (13)	1.392 (5)	1.398 (3)
N3–C7	1.367 (3)	1.3340 (16)	1.3494 (13)	1.368 (5)	1.348 (3)
O5–C7	1.211 (3)	1.2321 (16)	1.2252 (12)	1.220 (5)	1.207 (3)
Cl1–C8	1.749 (3)	1.7789 (14)	1.7626 (12)	1.775 (4)	1.779 (3)
Bond angle (°)					
C7–C8–Cl1	111.26 (18)	114.84 (9)	112.24 (8)	115.8 (3)	116.55 (17)
N3–C7–O5	123.5 (2)	122.96 (11)	123.62 (9)	124.5 (4)	125.6 (2)
O3–N2–O4	123.7 (2)	122.99 (11)	123.62 (10)	121.5 (5)	121.5 (2)
O5–C7–C8	123.4 (2)	118.88 (11)	122.84 (10)	117.7 (4)	117.1 (2)
Torsion angle (°)					
C4–N3–C7–C8	– 173.7 (2)	– 178.58 (11)	– 178.36 (10)	179.9 (4)	– 177.6 (2)
C4–N3–C7–O5	5.0 (4)	– 0.75 (19)	1.04 (17)	0.4 (7)	– 1.5 (4)
N3–C7–C8–Cl1	– 177.57 (18)	– 11.19 (15)	– 175.82 (8)	10.3 (5)	– 15.7 (3)
O5–C7–C8–Cl1	3.7 (4)	170.89 (10)	4.78 (15)	– 170.2 (3)	167.9 (2)

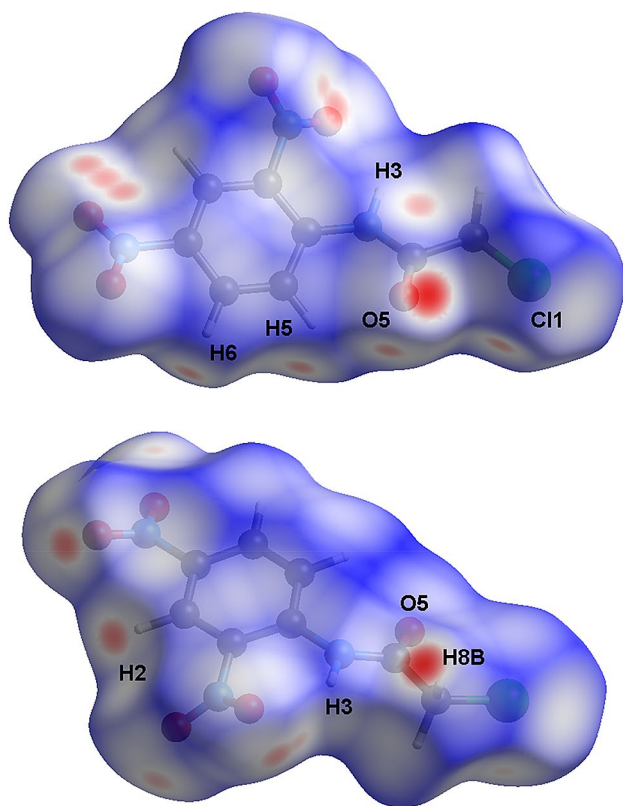


**Fig. 2** Two views of the three-dimensional Hirshfeld surface of the compound **1** plotted over  $d_{\text{norm}}$  in the range  $-0.2293$  to  $0.9126$  a.u

the equilibrium. The former, **1** might bind to DMF and DMSO using the hydrogen bonding interaction, and the latter, the NH proton of **1** can be loosened being deprotonated form in this solvent. The result signified that a new species of **1** appeared in the solution, as shown in Scheme 2. This evidence was evaluated by adding hydroxide ions to **1** in DMF solvent and further investigated by UV-vis and  $^1\text{H}$  NMR techniques. Upon addition of 1 equivalent  $\text{OH}^-$  to **1** in the DMF solvent, the signal of UV-vis spectra at 301 nm assigned to the normal form of **1** was decreased, while the one at 425 nm was enhanced, as shown in Fig. 6. Adding 2 equivalents of  $\text{OH}^-$ , the absorption band at 425 nm was significantly observed, while the other bands were vanished. It was indicated that the deprotonated form of **1** occurred in the solution exhibiting the UV-vis spectra at 425 nm, as shown in Fig. 6. The similar results are observed in the case of compound **1** in DMSO solvent. The other solvents showed only the band at 301 nm of the normal form of **1**. For further confirmation using  $^1\text{H}$  NMR, the addition of 1–2 equiv.  $\text{OH}^-$  to **1** in the mixing DMF and DMSO- $d_6$ , the NH proton at 11.77 ppm disappeared via the deprotonation process in Fig. 7. The ArH- and  $\text{CH}_2$ - protons moved to the upfield shift due to an increase of the electron density within the structure of compound **1**. These results indicated that a deprotonated

species was found in the solution. Note that, there were no deprotonated species in the nonpolar solvents.

## Computational Study

For a better understanding of the electronic properties of **1** (Fig. 8), the excitation energy, based on the first and second singlet–singlet electronic transitions were studied. Quantum calculation was investigated in order to understand the structural properties of the two forms of the **1**. The most stable structure for the normal form (N) and deprotonated form (DPT) molecule was investigated (Fig. 8). Both of their structures are corresponding to different orientations with respect to C–N and N–C distance.

The vertical first and second excitation energies were calculated by TD-DFT with PBE0 functional with the 6-311G(d,p) basis set, using PBE0/6-311G(d,p) optimized geometries at the global minimum of all molecules. The electronic properties in terms of excitation energy ( $E_{\text{ex}}$ ) and oscillator strength ( $f$ ) were then calculated. In Table 6, the theoretical results are in good agreement with the experimentally measured absorption maxima. The calculated absorption peaks at 300 nm and 392 nm should be attributed to the normal form (N) and deprotonated DPT-form, respectively, which are consistent with the experimental absorption spectra of the two forms, N-form and DPT-form, for **1**.

Table 6 shows that the  $S_0 \rightarrow S_1$  state of the N-form and DPT-form mainly corresponds to the orbital transition from the highest occupied molecular orbital (HOMO) to the lowest unoccupied molecular orbital (LUMO). Frontier molecular orbitals (MOs) are widely used to understand the nature of the excited states. The HOMO and LUMO of the N and DPT forms are presented in Fig. 9. The HOMO and LUMO are the  $\pi$  and  $\pi^*$  character, respectively. Hence, it is evident that the  $S_0 \rightarrow S_1$  state is  $\pi\pi^*$  feature. Molecular orbitals suggested that a  $\pi\pi^*$  state facilitates the deprotonated form. Note that, the electron density on the amine group in the LUMO in comparison to the HOMO is decreased, while the one on the carbonyl group is increased. The results of electronic spectra demonstrate that both the N-form and DPT-form of **1** could occur. The maximum absorption at 392 nm in DMF and DMSO related to the HOMO  $\rightarrow$  LUMO transitions of the deprotonated form. It was suggested that the deprotonated form was found in the polar solvent.

## Conclusion

2-Chloro-*N*-(2,4-dinitrophenyl)acetamide, **1** was successfully synthesized and fully characterized by NMR, MS, and EA. Although intermolecular hydrogen bonding is not observed in the crystal structure of **1**, the intramolecular H-bond is formed between the H atom of the amide

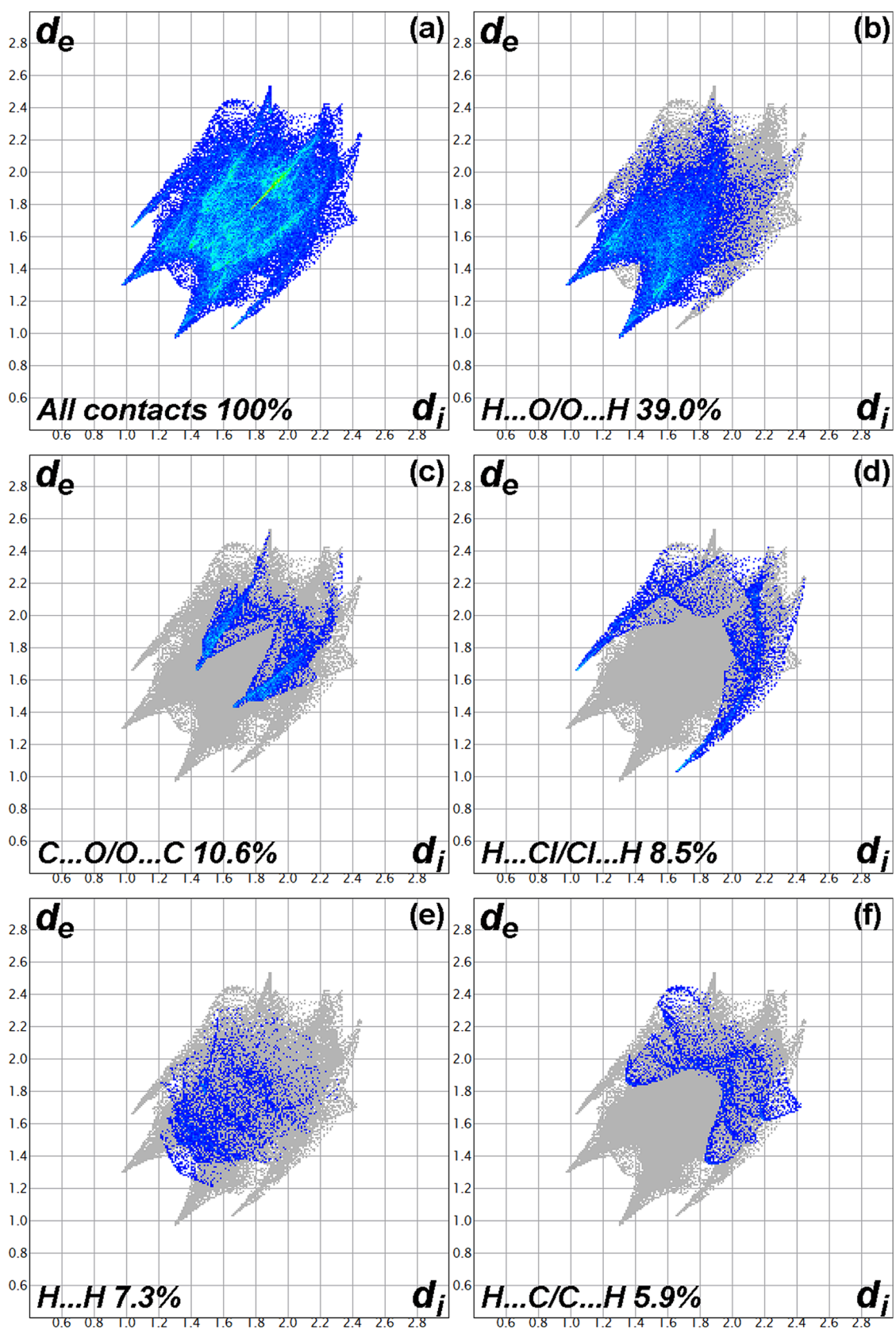


**Fig. 3** The full two-dimensional fingerprint plots for the title compound, showing **a** all interactions and those delineated into **b**  $H...O/O...H$  (39.0%), **c**  $C...O/O...C$  (10.6%), **d**  $H...Cl/Cl...H$  (8.5%), **e**  $H...H$  (7.3%), and **f**  $H...C/C...H$  (5.9%) interactions

**Fig. 4** 2-Chloro- *N*-(2,4-dinitrophenyl)acetamide **1** ( $1 \times 10^{-4}$  M) in organic solvents (from left to right:  $\text{CH}_2\text{Cl}_2$ ,  $\text{CHCl}_3$ ,  $\text{CH}_3\text{CN}$ ,  $\text{CH}_3\text{OH}$ , DMSO and DMF)



**Fig. 5** The UV–vis spectra of 2-chloro- *N*-(2,4-dinitrophenyl)acetamide **1** ( $1 \times 10^{-4}$  M) in different solvents

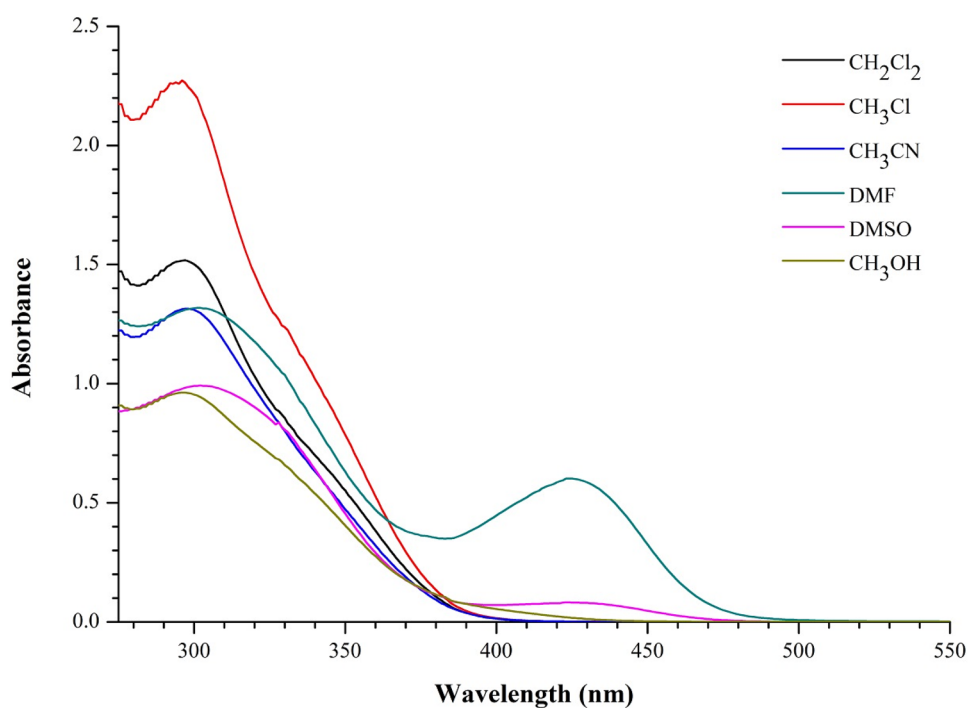


**Table 5** Absorption maximum (nm) and molar absorptivity of 2-chloro- *N*-(2,4-dinitrophenyl)acetamide **1** in different solvents

Solvents	$\lambda_{\text{max}}$ (nm)	Dielectric constant [23]	Molar absorptivity ( $\epsilon$ )
Dichloromethane	297	10.42	15,174.4
Chloroform	296	4.81	22,731.37
Acetonitrile	298	36.64	13,14,221
Methanol	296	32.60	9623.89
Dimethyl formamide	301 425	38.25 –	13,175.51 6018.88
Dimethyl sulfoxide	301 425	47.00 –	13,159.23 2617.3

group and the nitro group at the ortho position. The crystal structure of **1** is stabilized by C–H $\cdots$ O interactions. Hirshfeld surface analysis revealed that the significant contacts within the crystal of compound **1** are H $\cdots$ O/O $\cdots$ H (38.4%), C $\cdots$ O/O $\cdots$ C (10.4%), H $\cdots$ Cl/Cl $\cdots$ H (8.5%), H $\cdots$ H (7.7%), and H $\cdots$ C/C $\cdots$ H (6.2%) contacts. The optical properties of compound **1** in various solvents were investigated using UV–vis spectrophotometry. Compound **1** showed solvatochromic effects upon the variation of solvent polarity.

**Scheme 2** The normal and deprotonated forms of **1**

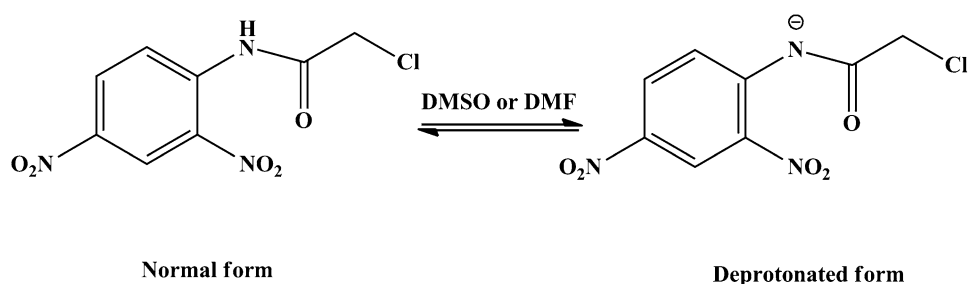
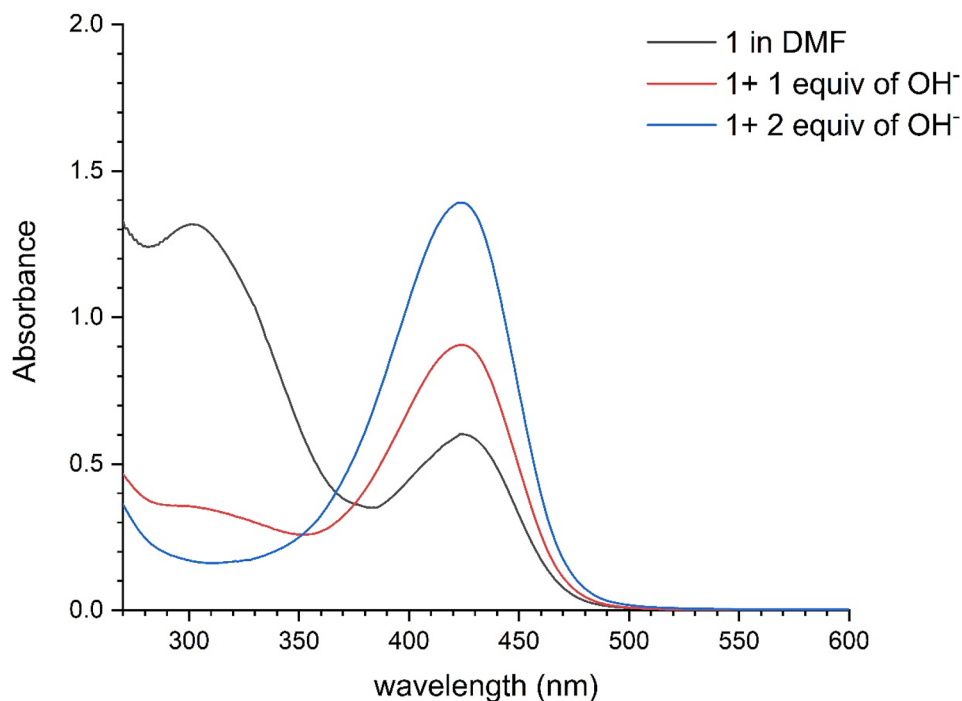


**Fig. 6** UV spectra of **1** ( $1 \times 10^{-4}$  M) without  $\text{OH}^-$  and **1** with different equivalent  $\text{OH}^-$  (tetrabutyl ammonium hydroxide was used for  $\text{OH}^-$ ) in DMF



Time-dependent DFT calculations (TD-DFT) suggest that the deprotonation process of compound **1** occurs in polar solvents such as DMF. Based on the DFT calculation, the deprotonation of **1** are responsible for the enhanced signal of the UV-vis band at 425 nm and correspondingly the change in the  $^1\text{H}$  NMR result.

**Acknowledgements** This research is supported by the Thailand Research Fund (MRG 5580182), Kasetsart University Research and Development Institute, and Department of Chemistry, Kasetsart University, and the Center of Excellent for Innovation in Chemistry (PERCH-CIC), Commission on Higher Education, Ministry of Education.

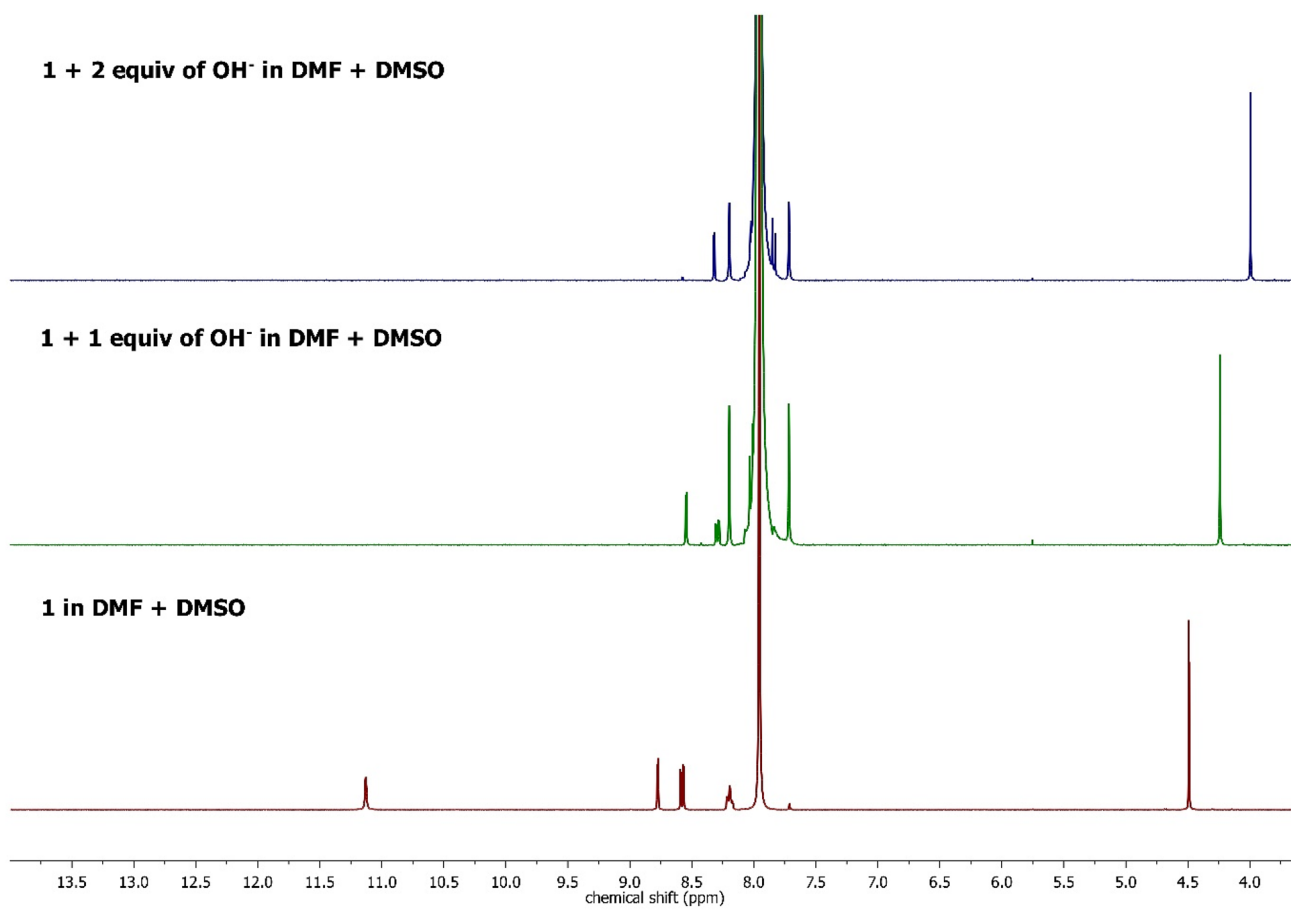


**Fig. 7** <sup>1</sup>H NMR spectra of **1** ( $1 \times 10^{-2}$  M) without OH<sup>-</sup> and **1** with different equivalent OH<sup>-</sup> (tetrabutyl ammonium hydroxide was used for OH<sup>-</sup>) in DMSO-*d*<sub>6</sub>

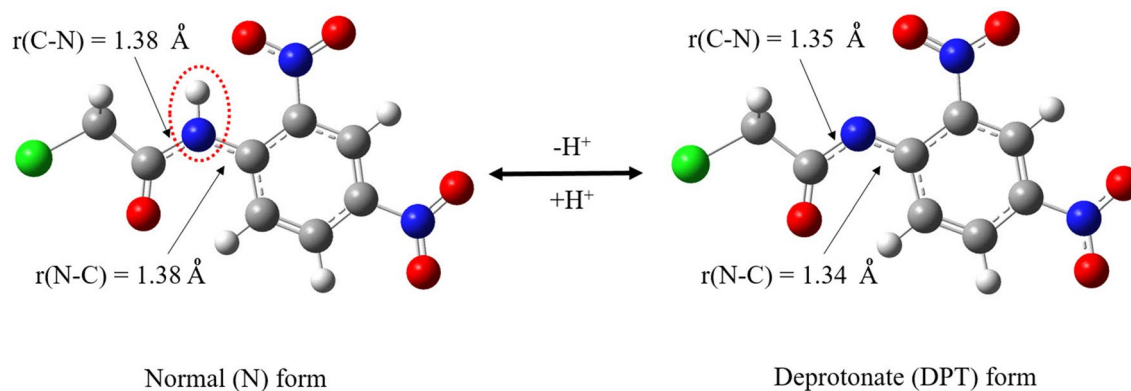
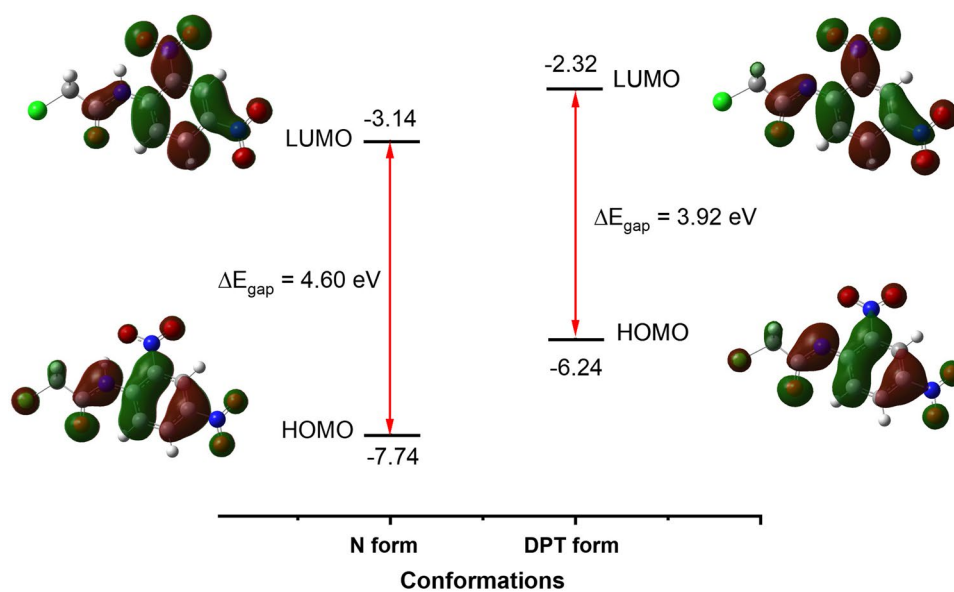


**Fig. 8** Structures of **1** of normal (N) and deprotonate forms (DPT)

**Table 6** Comparison of experimental and calculated absorbances; excitation energy, oscillator strength ( $f$ ), and major transition contributions of the N and DPT forms at PCM-TD-HSEH1PBE/6-311G(d,p) level in DMF solvent

States	Excitation energy			Major contribution
	eV	nm	$f$	
<b>N form</b>				
$S_0 \rightarrow S_1$	3.68	337	0.1223	HOMO $\rightarrow$ LUMO (94%)
$S_0 \rightarrow S_2$	3.95	314	0.0000	H-3 $\rightarrow$ L+1 (90%)
$S_0 \rightarrow S_3$	3.96	313	0.0000	H-6 $\rightarrow$ LUMO (53%)
$S_0 \rightarrow S_4$	4.13	300	0.4334	HOMO $\rightarrow$ L+1 (93%)
<b>DPT form</b>				
$S_0 \rightarrow S_1$	3.05	406	0.0001	H-1 $\rightarrow$ L+1 (89%)
$S_0 \rightarrow S_2$	3.16	392	0.1219	HOMO $\rightarrow$ LUMO (49%)
$S_0 \rightarrow S_3$	3.37	368	0.0001	H-1 $\rightarrow$ LUMO (87%)
$S_0 \rightarrow S_4$	3.44	361	0.6351	HOMO $\rightarrow$ LUMO (50%)

**Fig. 9** Frontier molecular orbitals of normal form (N) and deprotonate form (DPT) computed at PCM-TD-CAMB3LYP/6-311G (d,p) level



## Compliance with Ethical Standards

**Conflict of interest** The authors declare no conflict of interest.

## References

- Burrows AD, Mingo DM, White AJP, Williams DM (1996) *Chem Commun* 97–99
- Kolodziej HA, Orzeczkowski K, Szostak R, Freundlich P, Glowiak T, Sorriso S (1996) *J Mol Struct* 380:15–22
- Batsanov AS, Hubberstey P, Russell CE, Walton PH (1997) *J Chem Soc Dalton Trans* 15:2667–2672
- Balaban AT (1997) *J Am Chem Soc* 119:11558–11566
- Adamska EB, Jaskolski MJ, Brzezinski B (1999) *J Mol Struct* 475:167–173
- An H, Li Y, Wang E, Xiao D, Sun C, Xu L (2005) *Inorg Chem* 44:6062–6070
- M V, Kulkarni MV, Badami S, Yenagi J, Tonanavar J (2011) *Spectrochim Acta Part A* 84:137–143
- Ozeryanskii VA, Pozharskii AF (2013) *Tetrahedron* 69:2107–2112
- Fujio S, Hashizume D, Takamuki Y, Yasui M, Iwasaki F, Maki S, Niwa H, Ikeda H, Hirano T (2004) *Tetrahedron Lett* 45:8531–8534
- Umeda R, Nishida H, Otono M, Nishiyama Y (2011) *Tetrahedron Lett* 52:5494–5496
- Zimmermann LM, Nicolini J, Marini VG, Machado VG (2015) *Sens Actuators B Chem* 221:644–652
- Lee DY, Singh N, Jang DO (2011) *Tetrahedron Lett* 52:1368–1371
- Bagley MC, Lin Z, Pope SJA (2009) *Tetrahedron Lett* 50:6818–6822
- Guerra JPTA, Lindner A, Nicoletti CR, Marini VG, Silva M, Machado VG (2015) *Tetrahedron Lett* 56:4733–4736
- Qu Z, Li P, Zhang X, Wang E, Wang Y, Zhou P (2016) *J Lumin* 177:197–203
- Luo M, Wang S, Wang M, Huang S, Li C, Chen L, Ma X (2016) *Dyes Pigments* 132:48–57
- Singh AK, Singh RK (2015) *J Mol Struct* 1089:191–205
- Dolomanov OV, Bourhis LJ, Gildea RJ, Howard JAK, Puschmann H (2009) *J Appl Crystallogr* 42:339–341
- Sheldrick GM (2015) *Acta Crystallogr A* 71:3–8
- Sheldrick GM (2015) *Acta Crystallogr C* 71:3–8
- Macrae CF, Sovago I, Cottrell SJ, Galek PTA, McCabe P, Pidcock E, Platings M, Shields GP, Stevens JS, Towler M, Wood PA (2020) *J Appl Crystallogr* 53:226–235
- Yanai T, Tew DP, Handy NC (2004) *Chem Phys Lett* 393:51–57
- Frisch MJ et al (2009) *Gaussian 09*, revision B.01. Gaussian Inc., Wallingford
- Cammi R, Tomasi J (1995) *J Comput Chem* 16:1449–1458
- Zhao GJ, Han KL (2008) *Phys Chem* 9:1842
- Fawcett WFJ (1993) *Phys Chem* 97:9540–9546
- Andrews M, Ward BD, Laye RH, Kariuki BM, Pope SJA (2009) *Helv Chim Acta* 92:2159–2172
- Gowda BT, Foro S, Fuess H (2007) *Acta Crystallogr E* 63:o1975
- Zhang S-S, Xu L-L, Zou J, Bi S, Wen Y-H (2006) *Acta Crystallogr E* 62:o4478
- Gowda BT, Kožíšek J, Tokarčík M, Fuess H (2008) *Acta Crystallogr E* 64:o987
- Gowda BT, Foro S, Fuess H (2008) *Acta Crystallogr E* 64:o419
- Gowda BT, Foro S, Fuess H (2008) *Acta Crystallogr E* 64:o420
- Gowda BT, Foro S, Fuess H (2008) *Acta Crystallogr E* 64:o85
- Mongkolkeaw S, Songsasen A, Duangthongyou T, Chainok K, Suramitr S, Wattanathana W, Wannalarse B (2020) *Acta Crystallogr E* 76:594–598
- Hirshfeld FL (1977) *Theor Chim Acta* 44:129–138
- Spackman MA, Jayatilaka D (2009) *CrystEngComm* 11:19–32
- Turner MJ, McKinnon JJ, Wolff SK, Grimwood DJ, Spackman PR, Jayatilaka D, Spackman MA (2017) *Crystal Explorer 17*. The University of Western Australia, Perth
- McKinnon JJ, Jayatilaka D, Spackman MA (2007) *Chem Commun* 3814–3816
- Hiroki M, Takumi O, Satoshi O (2016) *Tetrahedron Lett* 57:3011–3015
- Sun Y, Wang G, Guo W (2009) *Tetrahedron* 65:3480–3485
- Yin Z, Jiang L, He J, Cheng JP (2003) *Chem Commun* 2326–2327
- Suramitr S, Hannongbua S, Wolschann P (2007) *J Mol Struct (THEOCHEM)* 807(1–3):109–119
- Wattanathana W, Nootsuwan N, Veranitisagul C, Koonsaeng N, Suramitr S, Laobuthee A (2016) *J Mol Struct* 1109:201–208
- Sriyab S, Gleeson MP, Hannongbua S, Suramitr S (2016) *J Mol Struct* 1125:532–539
- Fawcett WR (1993) *J Phys Chem* 97:9540–9546
- Catalán J, Palomar J, Díaz C, de Paz JLG (1997) *J Phys Chem* 101:5183–5189

**Publisher's Note** Springer Nature remains neutral with regard to jurisdictional claims in published maps and institutional affiliations.